

Lipidomic analysis of moss species *Bryum pseudotriquetrum* and *Physcomitrium patens* under cold stress

Yi Lu¹, Finnur Freyr Eiriksson², Margrét Thorsteinsdóttir², and Henrik Toft Simonsen¹

¹Danmarks Tekniske Universitet

²University of Iceland Faculty of Pharmaceutical Sciences

July 1, 2022

Abstract

As non-vascular plants, which lack lignin for protection, bryophytes support themselves in harsh environment by producing various chemicals. In response to cold stress, lipids play a crucial role in cell adaptation and energy storage. Specifically, bryophytes survive at low temperatures by producing very long-chain polyunsaturated fatty acids (vl-PUFAs). However, a systematic knowledge and comprehensive understanding of the cold acclimation of bryophytes is limited. To overcome this obstacle, we performed lipid profiling using ultra-high performance liquid chromatography-quadrupole time of flight mass spectrometry (UHPLC-QTOF-MS) of two moss species (*Bryum pseudotriquetrum* and *Physcomitrium patens*) cultivated at standard condition compared to those cultivated at cold stressed condition. The potential biomarkers were identified by multivariate statistical analysis in each species. In *B. pseudotriquetrum*, we found that the phospholipids and glycolipids increased significantly under cold stress, while storage lipids decreased. The accumulation of the lipids with high unsaturation degrees (i.e. at least one fatty acyl chain contains more than two double bonds) mostly appear in phospholipids and glycolipids. However, this trend cannot be observed in *P. patens*. This suggests that different moss species may undergo a different lipid metabolic pathway of cold adaptation. Our findings present a deeper understanding of how mosses are adapted to cold temperature and provide a basis for future studies.

Lipidomic analysis of moss species *Bryum pseudotriquetrum* and *Physcomitrium patens* under cold stress

Yi Lu^{1,2}, Finnur Freyr Eiriksson^{2,3}, Margrét Thorsteinsdóttir^{2,3} and Henrik Toft Simonsen^{1,*}

1. Department of Biotechnology and Biomedicine, Technical University of Denmark, Søtofts Plads 223, 2800 Kongens Lyngby, Denmark; yilu@dtu.dk (Y.L), hets@dtu.dk (H.T.S)
2. ArcticMass, Sturlugata 8, 101 Reykjavik, Iceland; finnur@arcticmass.is (F.F.E); margreth@hi.is (M.T)
3. Faculty of Pharmaceutical Sciences, University of Iceland, Hagi, Hofsvallagata 53, 107 Reykjavik, Iceland

* Correspondence: hets@dtu.dk

Abstract

As non-vascular plants, which lack lignin for protection, bryophytes support themselves in harsh environment by producing various chemicals. In response to cold stress, lipids play a crucial role in cell adaptation and energy storage. Specifically, bryophytes survive at low temperatures by producing very long-chain polyunsaturated fatty acids (vl-PUFAs). However, a systematic knowledge and comprehensive understanding of the cold acclimation of bryophytes is limited. To overcome this obstacle, we performed lipid profiling using ultra-high performance liquid chromatography-quadrupole time of flight mass spectrometry (UHPLC-QTOF-MS) of two moss species (*Bryum pseudotriquetrum* and *Physcomitrium patens*) cultivated at standard condition

compared to those cultivated at cold stressed condition. The potential biomarkers were identified by multivariate statistical analysis in each species. In *B. pseudotriquetrum*, we found that the phospholipids and glycolipids increased significantly under cold stress, while storage lipids decreased. The accumulation of the lipids with high unsaturation degrees (i.e. at least one fatty acyl chain contains more than two double bonds) mostly appear in phospholipids and glycolipids. However, this trend cannot be observed in *P. patens*. This suggests that different moss species may undergo a different lipid metabolic pathway of cold adaptation. Our findings present a deeper understanding of how mosses are adapted to cold temperature and provide a basis for future studies.

Keywords: lipidomics, cold stress, *Bryum pseudotriquetrum*, *Physcomitrium patens*, biomarker.

Introduction

Bryophytes have high chemical complexity and produce various metabolites, which indicate them as a promising resources in biotechnological applications such as pharmaceutical, cosmetics and food industry (Decker and Reski, 2020; Horn et al., 2021; Sabovljević et al., 2016). Bryophytes naturally produce high amounts of very long- chain polyunsaturated fatty acids (vl-PUFAs, ([?]²⁰ carbons, [?]² unsaturation degrees), including arachidonic acid (AA, 20:4) and eicosapentaenoic acid (EPA, 20:5) (Lu et al., 2019). The presence of vl-PUFAs is uncommon in vascular plants. Long-chain PUFAs ([?]¹⁸ carbons, [?]² unsaturation degrees), such as 18:2, 18:3, 20:4, 20:5, and 22:6, have been confirmed to be beneficial for human health for preventing cardiovascular disease, rheumatoid arthritis and inflammatory diseases (Calder and Yaqoob, 2009; Orsavova et al., 2015). The presence of PUFAs in mosses suggests mosses can be used as novel source of food supplement (Shanab et al., 2018). It is known that vl-PUFAs are essential for bryophytes to survive at low temperatures, some bryophytes even exist in very harsh environment such as the Arctic and Antarctic since they are capable of survive during hard frost (Glime, 2017). However, a comprehensive analysis of different moss species is lacking, and a detailed underlying mechanism of the adaptation of mosses to cold stress is still unknown.

Low (< 10) or freezing temperature usually leads to changes in the lipid composition and fatty acid desaturation in plants. The accumulation of vl-PUFAs can lower the solidification point of the cells and keep the plant membrane fluidity (Tarazona et al., 2015). However, the existing studies of mechanisms of cold stress mainly focus on higher plants and microalgae (Badea and Kumar Basu, 2009; Chen et al., 2013; de Freitas et al., 2019; Valledor et al., 2013). As an intermediate division between algae and vascular plants, bryophytes seem to be an overlooked group. Although the lipid compositions of different moss species were reported before to contain high contents of vl-PUFAs, most of the studies only examined their fatty acid profiles using conventional lipid analysis method such as thin-layer chromatography (TLC) or gas chromatography (GC) (Dembitsky et al., 1993; Gellerman et al., 1975; E. Hartmann et al., 1986; Pejin et al., 2012).

Physcomitrium patens is a model organism for studying non-seed plants (Rensing et al., 2020), and the full genome of *P. patens* has been published (Rensing et al., 2008). Compared to higher plants, *P. patens* has several enzymes such as $\Delta 6$ -desaturase, $\Delta 5$ -desaturase and $\Delta 6$ -elongase for desaturation and elongation for synthesis of C18-above fatty acids (Beike et al., 2014; Domergue et al., 2005). The lipidome of *P. patens* previously described consists of phospholipids including phosphatidylcholines (PC), phosphatidylethanolamines (PE), phosphatidylglycerols (PG), phosphatidylinositols (PI), and phosphatidic acid (PA), glycolipids including monogalactosyldiacylglycerols (MGDG), digalactosyldiacylglycerols (DGDG), and sulfoquinovosyldiacylglycerols (SQDG), storage lipids including diglyceride (DG) and triglyceride (TG), sphingolipids ceramides (Cer), free fatty acids (FA), and lysophospholipids (LPL) (Mikami and Hartmann, 2004; Resemann et al., 2021). Specifically, few studies confirmed that low temperature leads to the accumulation of the PUFAs in glycolipids (MGDG and DGDG) lipid class in bryophytes such as *Ceratodon purpureus* (Aro and Karunen, 1988). A very recent study in *P. patens* reported an increase in the levels of unsaturation of sphingolipids when exposing to cold temperature, and that mosses undergo a different response pathway than seed plants during low temperature acclimation (Resemann et al., 2021). However, the mechanism has not yet been confirmed in other moss species.

In this study, we present the lipid composition in two moss species, and report the changes in lipid composition under cold stress when cultivated at 25 and 10 by using lipidomics approach. *Bryum pseudotriquetrum* was selected for its fast growth rate at both standard conditions, and at cold temperature in liquid culture. Therefore, *B. pseudotriquetrum*, together with the model species *P. patens*, were chosen for investigating the lipid compositions and the lipid molecular species changes during cold adaptation. The lipid profiling was performed by ultra-high performance liquid chromatography-quadrupole time of flight mass spectrometry (UHPLC-QTOF MS) and data were analyzed by multivariate data analysis including principal components analysis (PCA) and projection to latent structures with discriminant analysis (PLS-DA). The potential biomarkers that are up-regulated and down-regulated under cold stress were identified, the relative concentrations of identified lipid molecular species and the total amount of each lipid class were quantified, and finally, the lipid physiology of mosses and their biological functions of cold adaptation are discussed.

Material and methods

1.

Chemicals

HPLC grade chloroform and methanol, LC-MS grade acetonitrile, isopropanol, ammonium acetate, tributylamine, and Potassium chloride (KCl, purity[?]99.0%) were purchased from Sigma-Aldrich (St. Louis, Missouri, USA). Hexakis(2,2,3,3-tetrafluoropropoxy)phosphazene were purchased from Apollo Scientific Ltd (Cheshire, UK). Glass tubes with PTFE coated caps were purchased from DWK Life Sciences (Staffordshire, UK). Ultra-pure water was obtained from a Milli-Q system (Sartorius, Göttingen, Germany).

In vitro cultivation

P. patens was obtained from Moss Stock Center at University of Freiburg, and sterilized *B. pseudotriquetrum* was obtained from Nils Cronberg, Lund University. Moss liquid culture was grown in Knop media (Reski and Abel, 1985), Prior to the experiment, moss culture was blended in sterile water for 30 s and inoculation started with a biomass concentration of 100-300 mg/L, 200 mL of blended moss liquid culture was inoculated in a 600 mL cell culture flasks (Corning, USA) and kept on a cell culture rocker. A 100 mL of biomass was harvested at day 21 for extraction of moss at room temperature and the rest of the biomass was left at 10 , and then harvested after another 24 h. The harvested biomass was filtered on a nylon filter and kept at -20 until extraction.

In the standard condition, the moss liquid cultures were maintained in a growth chamber with a temperature of 23 +- 1 degC, the light intensity was kept at 15 – 20 Wm⁻² as described by Pan et al. (2015). Cold stressed moss was kept in a growth chamber at 10 +- 1 with the same light intensity as the standard condition. Day/night cycle was 16h/8h in both conditions. Two biological replicates were prepared in each condition.

Internal standards

EQUISPLASH and DGTS d9 were purchased from Avanti Polar Lipids (Alabaster, Alabama, USA). A 10 µL of 100 µg/mL solution containing each internal standard (IS) was spiked to the samples. The ISs include: Phosphatidylcholine (PC) 15:0-18:1(d7), phosphatidylethanolamine (PE) 15:0-18:1(d7), phosphatidylglycerol (PG) 15:0-18:1(d7), phosphatidylinositol (PI) 15:0-18:1(d7), phosphatidylserine (PS) 15:0-18:1(d7), lysophosphatidylcholine (LPC) 18:1(d7), lysophosphatidylethanolamine (LPE) 18:1(d7), diglyceride (DG) 15:0-18:1(d7), triglyceride (TG) 15:0-18:1(d7)-15:0, MG 18:1(d7), cholesterol ester (CE) 18:1(d7), sphingomyelin (SM) d18:1/18:1(d9), sphingolipids ceramide (Cer) 18:1;2O/16:0(d7), and diacylglycerol-N,N,N-trimethylhomoserine (DGTS) d9.

Lipid extraction

Liquid cultures of mosses were harvested and filtered using Nylon cell strainers (pore size 70 μ m). The fresh moss material was ground in liquid nitrogen. 200 mg fresh frozen moss material was weighed into a glass tube; 3 mL chloroform/methanol (2:1, v/v) was added into the tube together with IS. The mixture was ultrasonicated for 20 min in dark, then vortexed on a vortex mixer before adding 0.75 mL 1M KCl. The mixture was vortexed again and centrifuged at 2000 g for 5 min at 4 °C. The organic phase was collected into a new glass tube by using a Pasteur pipette. The remaining mixture was washed twice with 1 mL chloroform, vortexed and centrifuged; the organic phases were combined and evaporated under nitrogen stream and stored at -20 until analysis. The dried lipid residue was re-suspended in 150 μ L of reconstitution solvent (one portion of chloroform/methanol (1:1, v/v) and nine portions of isopropanol/acetonitrile/water (2:1:1, v/v/v)). The solution was transferred to an Eppendorf tube and centrifuged at 13,000 g for 5 min at room temperature, 100 μ L of the supernatant was transferred to an HPLC vial with a glass insert for analysis. Quality control (QC) was prepared by pooling 10 μ L aliquots of all samples.

Lipid quantification and recovery

Relative quantification of individual lipid molecular species was performed by using internal standards (see section 2.3) representing their own lipid classes. Lipid recovery was calculated by spiking the internal standards before (pre-spike) and after (post-spike) lipid extraction. For lipids that generate more than one form of ions, the most abundant ion form was chosen for relative quantification.

UHPLC-QTOF-MS analysis

UHPLC-QTOF-MS was performed on an Agilent Infinity 1290 UHPLC system (Agilent Technologies, Santa Clara, CA, USA) coupled with Agilent 6545 QTOF MS with Dual Jet Stream ESI source. Samples were separated on an ACQUITY UPLC HSS T3 column (100 \AA , 1.8 μ m, 2.1 mm X 150 mm). The flow rate was 0.4 mL/min and the column temperature was 55 °C. Solvent A consists of acetonitrile/H₂O (60:40, v/v) and solvent B was isopropanol/acetonitrile (90:10, v/v), both supplied with 10 mM ammonium acetate. Linear gradient started from 40% solvent B and increased to 100% B in 10 min, and held at 100% B for 2 min, then reconditioned to 40% B in 2.5 min. Total analysis time was 15 min. The auto sampler temperature was 8 °C. Injection volume was 2 μ L in positive ionization (ESI+) mode and 5 μ L in negative ionization (ESI-) mode. Mass range was 100-1700 Da for MS scan and 30 – 1700 Da for MS/MS scan. Data were recorded in positive and negative ionization mode with an acquisition rate of 10 spectra/s in centroid profiles. Fragmentations were recorded with fixed collision energies of 10, 20 and 40 eV with maximum three precursors per cycle. Lock mass solution 1 μ M tributylamine and 10 μ M hexakis(2,2,3,3-tetrafluoropropoxy)phosphazene with m/z 186.2216 and 922.0098 [M+H]⁺ in ESI+ mode and m/z 966.0012 [M+COOH]⁻ in ESI- mode.

Data analysis

Agilent MassHunter Qualitative Analysis (B.07.00) was used for preliminary data quality checking and for calculation of the internal standards. The raw data files were imported directly to MS-DIAL (version 4.60) for further data analysis (peak peaking, deconvolution, compound identification and alignment). Data normalization was achieved by calculating relative concentrations by using the internal standard representing the same lipid class. The alignment result was imported to SIMCA 17 (Umetrics AB, Sweden) for principal components analysis (PCA) and projection to latent structures with discriminant analysis (PLS-DA). Data was pareto-scaled and log₂-transformed. T-test was performed for calculating statistical significance of lipid concentration changes.

Results

- 1.

Standard calibration and recovery

To perform relative quantification of detected lipids, calibration curves of each IS were made with at least six concentration points (Table 1). Eight ISs were used for quantification in ESI+ mode and five in ESI- mode. The linear ranges vary from 0.125 to up to 40 ug/mL with all R² exceed 0.99.

The recovery of the ISs was tested by comparing the peak areas of their corresponding m/z before (pre-spike) and after (post-spike) extraction procedure. Most of the internal standards showed more than 85% recovery (Supplementary figure S5). PI 15:0-18:1(d7) had with the lowest recovery in both ESI+ and ESI- mode (73% and 78%, respectively), as expected (Aldana et al., 2020).

Lipid compositions in *B. pseudotriquetrum* and *P. patens*

B. pseudotriquetrum was tested for its *in vitro* growth ability, and it showed relatively high growth rate both under room temperature and under cold temperature. Thus, this species was chosen for evaluation of lipid profiling under cold stress together with the model species *P. patens* to unravel the lipid metabolisms in different moss species.

To review the lipid composition in *B. pseudotriquetrum* and *P. patens*, the identified lipids were classified accordingly to their lipid classes in ESI+ and ESI- mode, the lipid classes and the corresponding numbers of lipid metabolites are shown in Figure 1. In total, 204 features in ESI+ mode and 176 in ESI- mode, were identified in the whole dataset with high quality MS² spectras, including different adducts of the same lipid molecular species. After selecting the adduct with the most abundant intensity of a lipid molecular species, 178 lipid metabolites were detected in ESI+ mode and 143 in ESI- mode in *B. pseudotriquetrum*, whereas 159 lipid metabolites were detected in ESI+ mode and 133 in ESI- mode in *P. patens*. Similar lipid metabolites could be found in both species, but the amount of each lipid metabolite varies (Supplementary Figure S2).

The major lipids found in both moss species are phospholipids such as PC, PE, PG and PI, glycolipids MGDG, DGDG and SQDG, signaling lipid Cer, and storage lipids DG and TG. Two unusual lipid classes PMeOH and sulfonolipids were detected in both moss species, along with considerable amounts of v1-PUFAs detected in ESI- mode as free fatty acids (FA). The most abundant FA were in *B. pseudotriquetrum* 20:4 and 20:5, and in *P. patens* 16:0 (Supplementary Figure S2). In addition, longer-chain-FAs with more than 20 carbons, such as saturated or mono-saturated C22-C25 FAs, were detected in both moss species.

Identification of biomarkers under cold stress

To discover the potential biomarkers of *B. pseudotriquetrum* and *P. patens*, chemometric approaches were applied by using unsupervised PCA and supervised PLS-DA. First, PCA plots were generated to visualize the group information and to monitor the quality of the data (Supplementary Figure S1). The two moss species show clear separation and the quality control samples are clustered tightly together, indicating that the batch is of good quality. *B. pseudotriquetrum* shows higher inter-species variations between room temperature and cold temperature in ESI+ mode, this may indicate that *B. pseudotriquetrum* has a stronger response to cold stress than *P. patens*.

In order to discriminate the samples that belong to room temperature and under cold stress in each species, individual PLS-DA models were built for *B. pseudotriquetrum* and *P. patens* for ESI+ and ESI- mode dataset, respectively (Figure 2). All models showed clear separation of two groups of samples with high cumulative X and Y matrix variations (R²X and R²Y, respectively) and high predictability (Q²). As seen in Figure 4A, the PLS-DA model resulted in one predictive and two orthogonal components. A total X variance (R²X) of 0.449 can be explained, and the predicted variance R²Y was 0.961. The predictive ability Q²Y = 0.676, which indicates good predictability (Eriksson et al., 2006). To test the validity of the models, permutation tests with 999 iterations were performed for all four models. The permutation tests are shown in Supplementary Figure S3. Normally, a well-fitted model should have an intercept of R² smaller than 0.4 and Q² should be smaller than 0.05. However, this is hard to achieve with too few samples in the model. In

this case, the slope of R2 and Q2 should be larger than 0. In this work, all of the Q2 intercepts were below 0 but the R2 are greater than 0.4, the slopes of both R2 and Q2 were larger than 0, thus, the models can be considered valid.

The potential biomarkers were screened based on three criteria (fold change of larger than 2 or smaller than 0.5, $p < 0.05$, and $VIP > 1$). The lipid molecular species that fulfilled all three criteria were designated as biomarkers for cold stress (Figure 3). In *B. pseudotriquetrum*, several membrane lipids (mostly PC, such as PC 34:2, and PC 18:2_20:4, and PG 16:0_16:0, PI 34:2, as well as most of the 34-38 carbons MGDG and DGDG with C16-18 FAs, showed an increase under cold stress. In ESI- mode, all identified PMeOH lipids were up-regulated under cold stress, together with PE 16:0_18:2, PE 16:0_20:4, and PI 16:0_18:2. The storage lipids, including DG and TG, in contrast, are down-regulated under cold stress. In *P. patens*, most of the TG lipids decreased under cold stress, but several DG lipids (e.g., DG 16:0_18:1, DG 16:0_20:3, and DG 18:1_18:3) and PG (PG 16:1_18:3 and PG 16:1_18:2) increased.

Four out of five identified PMeOH lipids (PMeOH 16:0_18:1, PMeOH 16:0_18:2, PMeOH 16:0_18:3, and PMeOH 16:0_20:4) showed significant increase in both moss species. As mentioned in the previous chapter, the choline head group from PC can react with methanol when phospholipase D is active and the final product is PMeOH and choline. However, we speculate the PMeOH is also produced endogenously in *P. patens* since the total amount of PC decreased while total amount of PMeOH increased.

Discussion

1.

Calibration and recovery

The standards used for the study was well recovered during the extraction and were chosen based on a preliminary study on the lipid profil. Welti et al. (2002) used hydrogenated MGDG and DGDG as internal standards for plant lipid profiling since those lipids do not exist in *Arabidopsis thaliana*. However, hydrogenated glycolipids are not suitable for using as internal standards for bryophytes because we have detected DGDG 32:0 (16:0_16:0) and SQDG 32:0 (16:0_16:0) produced by *P. patens* in our test run. Therefore, a deuterated glycolipid DGTS (d9) was used for glycolipids (MGDG, DGDG, and SQDG) quantification.

Lipid composition and changes during cold stress

The major phospholipids, signaling lipids and storage lipids found in both moss species are common lipid classes also found in algae, higher plants and bryophytes (Chen et al., 2013; Conde et al., 2021; Okazaki and Saito, 2018; Vu et al., 2014). The unusual lipid class PMeOH also detected in both moss species is suspected to be an artifact from lipid extraction when using methanol (Roughan et al., 1978). The PMeOH lipid was identified by its characteristic m/z 110.981 (CH4OP-) in ESI- mode, which corresponds to the head group of a phosphatidic acid with a methyl group added to the phosphate, an example of the MS/MS spectrum of PMeOH 16:0_18:2 is shown in Supplementary Figure S4. The precursor of PMeOH is generally believed to be PC, which reacts with methanol in the presence of phospholipase D (PLD) by transphosphatidylation. Tsugawa et al. (2019) analyzed the lipid compositions of nine algal species, but only detected several PMeOH lipids in algae *Euglena gracilis*, even if all algal species were extracted with the same method. In our study, the moss materials were kept at -20 as soon as possible after harvest, and were ground in liquid nitrogen to quench the lipid metabolism, before lipid extraction. Despite these precautions, PMeOH was still detected, and it is still unclear under which circumstances these formations of PMeOH occurred. Furthermore, differences of the cold response are showed in PC and PMeOH, e.g., PC 16:0_18:2 decreased in cold stress in *P. patens*, whereas PMeOH 16:0_18:2 increased (Supplementary Figure S2). The different cold response of PC and PMeOH suggests PMeOH may not only be an artifact of extraction, but could also be a *de novo* biosynthetic pathway of *P. patens*. This could be confirmed by using another extraction solvent, e.g., ethanol, methyl-tert butyl ether (MTBE), dichloromethane (CH₂Cl₂), in future experiments.

Another unusual lipid class, sulfonolipids (SLs, or N-acyl-capsine) again detected in both moss species are structurally related to ceramides but has a sulfonic acid group in the sphingoid base (Walker et al., 2017). Five SLs and oxidized SLs (O-acetylated SL) were identified as [M-H]⁻ adducts by their characteristic m/z 79.958, which represents the sulfite group, and a neutral loss of the fatty acyl from the sphingoid base, an example of MS/MS spectrum of SL (17:0;0/17:1) is shown in Supplementary Figure S4. SLs were only described in diatoms (Anderson et al., 1978) and some bacterial species before (Walker et al., 2017). SL is likely produced by N-acylation of its precursor capsine with fatty acids (Godchaux and Leadbetter, 1980).

The presence of SLs may suggest a new biosynthetic pathway of bryophytes; however, it could also be bacterial contamination in the liquid culture, even if SLs have not been detected by non-axenic materials previously (Lu et al., 2021).

The detection of considerable amounts of vl-PUFAs in both moss species, including FA's longer than 20 carbons is in agreement with (Beike et al., 2014), that also described 24:0, 25:0, and 26:0 FAs in several moss species. However, the level of total amount of FA in *B. pseudotriquetrum* did not change under cold stress, which could have been expected. Thus, there biosynthesis might not be regulated by temperature but be a consistent production that ensure a constant resistant to temperature changes.

Although *B. pseudotriquetrum* and *P. patens* have a similar lipid composition in terms of the lipid molecular species, the individual lipid molecular species vary in a quantitative level (Figure 2). Similar quantities of phospholipids (such as PC, PE, PG, PI, and PA) were detected in both species, but *B. pseudotriquetrum* has significant higher amounts of storage lipids (DG and TG), signaling lipid Cer and FA. In contrast, *P. patens* has higher amounts of glycolipids (MGDG, DGDG, and SQDG) compared to *B. pseudotriquetrum*. The high concentration of glycolipids in *P. patens* are mostly contributed by C16-18 carbon lipids such as MGDG 16:2_18:2, MGDG 16:2_18:3, MGDG 16:3_18:3, DGDG 16:0_18:2, and SQDG 16:0_18:2. *B. pseudotriquetrum*, on the other hands, contains high amounts of 20:4-containing lipids such as DG 16:0_20:4, DG 20:4_20:4, TG 18:3_20:4_20:4, TG 20:4_20:4_20:4, and FA 20:4.

In *B. pseudotriquetrum*, phospholipids PC, PG, PI, and glycolipids MGDG, showed significant increase (Figure 4). In the molecular species level, accumulations of PC with at least one polyunsaturated fatty acyl chain, such as PC 34:2 (16:0_18:2), PC 34:3 (16:0_18:3), PC 36:4 (16:0_20:4), and PC 38:7 (18:3_20:4), were observed under cold stress, while lipid species with two saturated or mono-saturated fatty acyl chains, such as PC 32:0 (16:0_16:0), and PC 32:1 (16:0_16:1) decreased (Supplementary Figure S2). Lysophospholipids are minor components of plant membranes and act as signaling mediators. In *B. pseudotriquetrum*, LPC 16:0 and 20:4 also showed increase under cold stress. Zhang et al. 2013 found several characteristic lysophospholipids increase in *Arabidopsis thaliana* in response to low temperature. The generation of lysophospholipids is caused by phospholipase A, which releases a fatty acyl chain from glycerophospholipid (Hou et al., 2016). Similar to PC, MGDG with higher degrees of unsaturation levels, such as MGDG 36:6 (18:3_18:3), MGDG 34:6 (16:3_18:3), and MGDG 38:6 (18:2_20:4), increased under cold stress, while MGDG 34:1 (16:0_18:1) decreased. Those findings are generally consistent with previous studies of higher plants or algae (Chen et al., 2013; Gao et al., 2019; Resemann, 2018; Wang et al., 2006). Wang et al. 2006 reported similar results of *Arabidopsis thaliana* and concluded that several phospholipases are more active when exposed to cold temperature.

It is known that vl-PUFAs provide freezing tolerance for the mosses (Glime, 2017; Hansen and Rossi, 1991; E Hartmann et al., 1986; Lu et al., 2019), one may expect to find higher PUFAs in association with phospholipids and glycolipids. However, there are some exceptions observed in *B. pseudotriquetrum*, such as PG 32:0(16:0_16:0) and DGDG 32:0 (16:0_16:0), which increased under cold stress, whereas DGDG 40:8 (20:4_20:4) decreased.

The lipid metabolism of *P. patens* was described before (Mikami and Hartmann, 2004), but the knowledge of lipid metabolism of how *P. patens* respond to cold stress is still limited. A recent study investigated the lipid changes of wild type *P. patens* under cold stress (Resemann, 2018), the author found that polyunsaturated C16 and C18 FAs decreased, but vl-PUFAs (C20 and above) accumulated in phospholipids and glycolipids.

In our study, we found the 20:4 and 20:5 containing lipids accumulated mostly in PC, MGDG and DG in *P. patens* under cold stress (Figure 3, Supplementary Figure S2).

Plants usually contain a larger amount of PG than animals and other non-photosynthetic organisms, since PG is located not only on cellular membranes, but also on chloroplast membranes (Walti et al., 2003). Interestingly, PG is the only lipid class in which no FA 20:4 and above were observed. This result matches with Resemann 2018, who studied the lipid composition of *P. patens*. However, the reason why PG lipid class contains no FA 20:4 remains unclear.

PE remained at the same level after exposing to cold temperature in both moss species; this may indicate that PE is not actively involved in cold adaptation in mosses, or that the temperature was not low enough to cause a significant change to PE. This is similar to the results of Hartmann et al. (1986), who reported that the AA and EPA contents in PE lipid fraction of moss *Leptobryum* remained the same level after 20 days of cold stress, although the ratio between AA and EPA decreased during the time.

Total content of TG decreased significantly in both *B. pseudotriquetrum* and *P. patens* (Figure 4), which indicates the TG breaks down in the moss cells when exposed to cold stress (Chen et al., 2013), and use the FAs released from TG for synthesis of phospholipids and glycolipids. Resemann (2018) reported a slight increase of TG in wild type *P. patens* under cold stress at 4 °C. However, they have conducted a much longer stress period (7 days), we therefore assume the TG synthesis undergoes a decrease when exposed to acute cold stress (24 h), then recovers gradually afterwards. The regulation of TG in plants is not yet well-studied, possibly due to the fact that TG lipids have complex structures and several combinations of fatty acyls, which may cause false identifications based on their MS/MS spectrums (Tsugawa et al., 2019).

Conclusion

By using mass spectrometry based lipidomic approach we identified hundreds of lipids with high quality MS/MS spectrums in moss *B. pseudotriquetrum* and *P. patens*. The lipidomes of *Bryum pseudotriquetrum* is reported the first time. Unusual lipids such as sulfonolipids, phosphatidylmethanol, and hydrogenated glycolipid DGDG 32:0, were found the first time in both moss species. *Bryum pseudotriquetrum* and *Physcomitrium patens* respond differently to cold stress. Multivariate statistical analysis of the LC-MS data from *B. pseudotriquetrum* and *P. patens*, indicated that 25 and 26 lipids were found to be up-regulated and 43 and 69 lipids were downregulated during cold stress, respectively. Overall, this work provides further insight of the cold stress adaptation in bryophytes with specific focus on the lipid metabolism.

Acknowledgement

This study is funded by Marie Skłodowska-Curie Actions, Innovative Training Networks under European Union Horizon 2020 programme under grant agreement No. 765115—MossTech.

Conflict of interest

The authors declare no conflict of interest.

Author contributions

Conceived and designed the experiments: YL and HTS. Performed the experiments: YL. Analyzed the data: YL. Wrote the manuscript: YL. Revised the manuscript: FFE, MT, and HTS. All authors approved the final manuscript.

Data Availability Statement

All data that support the findings of this study are available at DTU data repository, Lu et al (2022): Cold stress paper. Technical University of Denmark. Dataset. <https://doi.org/10.11583/DTU.20198699>.

References

- Aldana, J., Romero-Otero, A., Cala, M.P., 2020. Exploring the Lipidome: Current Lipid Extraction Techniques for Mass Spectrometry Analysis. *Metabolites* 10, 231. <https://doi.org/10.3390/metabo10060231>
- Anderson, R., Kates, M., Volcani, B.E., 1978. Identification of the sulfolipids in the non-photosynthetic diatom *nitzschia alba*. *Biochim. Biophys. Acta - Lipids Lipid Metab.* 528, 89–106. [https://doi.org/10.1016/0005-2760\(78\)90055-3](https://doi.org/10.1016/0005-2760(78)90055-3)
- Aro, E.-M., Karunen, P., 1988. Effects of hardening and freezing stress on membrane lipids and CO₂ fixation of *Ceratodon purpureus* protonemata. *Physiol. Plant.* 74, 45–52. <https://doi.org/10.1111/J.1399-3054.1988.TB04939.X>
- Badea, C., Kumar Basu, S., 2009. The effect of low temperature on metabolism of membrane lipids in plants and associated gene expression. *Plant Omi. J. South. Cross Journals*©2009 2, 78–84.
- Beike, A.K., Jaeger, C., Zink, F., Decker, E.L., Reski, R., 2014. High contents of very long-chain polyunsaturated fatty acids in different moss species. *Plant Cell Rep.* 33, 245–254. <https://doi.org/10.1007/s00299-013-1525-z>
- Calder, P.C., Yaqoob, P., 2009. Omega-3 polyunsaturated fatty acids and human health outcomes. *BioFactors* 35, 266–272. <https://doi.org/10.1002/biof.42>
- Chen, D., Yan, X., Xu, J., Su, X., Li, L., 2013. Lipidomic profiling and discovery of lipid biomarkers in *Stephanodiscus* sp. under cold stress. *Metabolomics* 9, 949–959. <https://doi.org/10.1007/s11306-013-0515-z>
- Conde, T.A., Couto, D., Melo, T., Costa, M., Silva, J., Domingues, M.R., Domingues, P., 2021. Polar lipidomic profile shows *Chlorococcum amblystomatis* as a promising source of value-added lipids. *Sci. Rep.* 11, 4355. <https://doi.org/10.1038/s41598-021-83455-y>
- de Freitas, G.M., Thomas, J., Liyanage, R., Lay, J.O., Basu, S., Ramegowda, V., do Amaral, M.N., Benitez, L.C., Bolacel Braga, E.J., Pereira, A., 2019. Cold tolerance response mechanisms revealed through comparative analysis of gene and protein expression in multiple rice genotypes. *PLoS One* 14, e0218019. <https://doi.org/10.1371/journal.pone.0218019>
- Decker, E.L., Reski, R., 2020. Mosses in biotechnology. *Curr. Opin. Biotechnol.* 61, 21–27. <https://doi.org/10.1016/j.copbio.2019.09.021>
- Dembitsky, V.M., Rezanka, T., Bychek, I.A., Afonina, O.M., 1993. Polar lipid and fatty acid composition of some bryophytes. *Phytochemistry* 33, 1009–1014. [https://doi.org/10.1016/0031-9422\(93\)85013-H](https://doi.org/10.1016/0031-9422(93)85013-H)
- Domergue, F., Abbadi, A., Zähringer, U., Moreau, H., Heinz, E., 2005. In vivo characterization of the first acyl-CoA $\Delta 6$ -desaturase from a member of the plant kingdom, the microalga *Ostreococcus tauri*. *Biochem. J.* 389, 483–490. <https://doi.org/10.1042/BJ20050111>
- Eriksson, L., Kettaneh-Wold, N., Trygg, J., Wikström, C., Wold, S., 2006. Multi- and Megavariate Data Analysis : Part I: Basic Principles and Applications. Umetrics Inc, Department of Chemistry, Faculty of Science and Technology, Umea University.
- Gao, X., Liu, W., Mei, J., Xie, J., 2019. Quantitative Analysis of Cold Stress Inducing Lipidomic Changes in *Shewanella putrefaciens* Using UHPLC-ESI-MS/MS. *Molecules* 24, 4609. <https://doi.org/10.3390/molecules24244609>
- Gellerman, J.L., Anderson, W.H., Richardson, D.G., Schlenk, H., 1975. Distribution of arachidonic and eicosapentaenoic acids in the lipids of mosses. *Biochim. Biophys. Acta - Lipids Lipid Metab.* 388, 277–290. [https://doi.org/10.1016/0005-2760\(75\)90133-2](https://doi.org/10.1016/0005-2760(75)90133-2)
- Glime, J.M., 2017. Volume 1, Chapter 10-2: Temperature: Cold.

- Godchaux, W., Leadbetter, E.R., 1980. Capnocytophaga spp. contain sulfonolipids that are novel in pro-caryotes. *J. Bacteriol.* 144, 592–602. <https://doi.org/10.1128/JB.144.2.592-602.1980>
- Hansen, C.E., Rossi, P., 1991. Effects of culture conditions on accumulation of arachidonic and eicosapentaenoic acids in cultured cells of *Rhytidiadelphus squarrosus* and *Eurhynchium striatum*. *Phytochemistry* 30, 1837–1841. [https://doi.org/10.1016/0031-9422\(91\)85024-T](https://doi.org/10.1016/0031-9422(91)85024-T)
- Hartmann, E., Beutelmann, P., Vandekerkhove, O., Euler, R., Kohn, G., 1986. Moss cell cultures as sources of arachidonic and eicosapentaenoic acids. *FEBS Lett.* 198, 51–55. [https://doi.org/10.1016/0014-5793\(86\)81183-8](https://doi.org/10.1016/0014-5793(86)81183-8)
- Hartmann, E., Beutelmann, P., Vandekerkhove, O., Euler, R., Kohn, G., 1986. Moss cell cultures as sources of arachidonic and eicosapentaenoic acids. *FEBS Lett.* 198, 51–55. [https://doi.org/10.1016/0014-5793\(86\)81183-8](https://doi.org/10.1016/0014-5793(86)81183-8)
- Horn, A., Pascal, A., Lončarević, I., Volpatto Marques, R., Lu, Y., Miguel, S., Bourgaud, F., Thorsteinsdóttir, M., Cronberg, N., Becker, J.D., Reski, R., Simonsen, H.T., 2021. Natural Products from Bryophytes: From Basic Biology to Biotechnological Applications. *CRC. Crit. Rev. Plant Sci.* 40, 191–217. <https://doi.org/10.1080/07352689.2021.1911034>
- Hou, Q., Ufer, G., Bartels, D., 2016. Lipid signalling in plant responses to abiotic stress. *Plant. Cell Environ.* 39, 1029–1048. <https://doi.org/10.1111/pce.12666>
- Lu, Y., Eiriksson, F.F., Thorsteinsdóttir, M., Simonsen, H.T., 2021. Effects of extraction parameters on lipid profiling of mosses using UPLC-ESI-QTOF-MS and multivariate data analysis. *Metabolomics* 17, 96. <https://doi.org/10.1007/s11306-021-01847-7>
- Lu, Y., Eiriksson, F.F., Thorsteinsdóttir, M., Simonsen, H.T., 2019. Valuable Fatty Acids in Bryophytes—Production, Biosynthesis, Analysis and Applications. *Plants* 8, 524. <https://doi.org/10.3390/plants8110524>
- Mikami, K., Hartmann, E., 2004. Lipid Metabolism in Mosses, in: *New Frontiers in Bryology*. Springer Netherlands, Dordrecht, pp. 133–155. https://doi.org/10.1007/978-0-306-48568-8_8
- Okazaki, Y., Saito, K., 2018. Plant Lipidomics Using UPLC-QTOF-MS, in: *Methods in Molecular Biology (Clifton, N.J.)*. pp. 157–169. https://doi.org/10.1007/978-1-4939-7819-9_11
- Orsavova, J., Misurcova, L., Vavra Ambrozova, J., Vicha, R., Mlcek, J., 2015. Fatty acids composition of vegetable oils and its contribution to dietary energy intake and dependence of cardiovascular mortality on dietary intake of fatty acids. *Int. J. Mol. Sci.* 16, 12871–12890. <https://doi.org/10.3390/ijms160612871>
- Pan, X.-W., Han, L., Zhang, Y.-H., Chen, D.-F., Simonsen, H.T., 2015. Sclareol production in the moss *Physcomitrella patens* and observations on growth and terpenoid biosynthesis. *Plant Biotechnol. Rep.* 9, 149–159. <https://doi.org/10.1007/s11816-015-0353-8>
- Pejin, B., Vujisić, L., Sabovljević, M., Tešević, V., Vajs, V., Vujisic, L., Sabovljevic, M., Tesevic, V., Vajs, V., 2012. The moss *Mnium hornum*, a promising source of arachidonic acid. *Chem. Nat. Compd.* 48, 120–121. <https://doi.org/10.1007/s10600-012-0175-7>
- Rensing, S.A., Goffinet, B., Meyberg, R., Wu, S.-Z., Bezanilla, M., 2020. The Moss *Physcomitrium* (*Physcomitrella*) *patens*: A Model Organism for Non-Seed Plants. *Plant Cell* 32, 1361–1376. <https://doi.org/10.1105/tpc.19.00828>
- Rensing, S.A., Lang, D., Zimmer, A.D., Terry, A., Salamov, A., Shapiro, H., Nishiyama, T., Perroud, P.-F., Lindquist, E.A., Kamisugi, Y., Tanahashi, T., Sakakibara, K., Fujita, T., Oishi, K., Shin-I, T., Kuroki, Y., Toyoda, A., Suzuki, Y., Hashimoto, S. -i., Yamaguchi, K., Sugano, S., Kohara, Y., Fujiyama, A., Anterola, A., Aoki, S., Ashton, N., Barbazuk, W.B., Barker, E., Bennetzen, J.L., Blankenship, R., Cho, S.H., Dutcher, S.K., Estelle, M., Fawcett, J.A., Gundlach, H., Hanada, K., Heyl, A., Hicks, K.A., Hughes, J., Lohr, M., Mayer, K., Melkozernov, A., Murata, T., Nelson, D.R., Pils, B., Prigge, M., Reiss, B., Renner, T., Rombauts,

S., Rushton, P.J., Sanderfoot, A., Schween, G., Shiu, S.-H.S.-H.S.-H., Stueber, K., Theodoulou, F.L., Tu, H., Van de Peer, Y., Verrier, P.J., Waters, E., Wood, A., Yang, L., Cove, D., Cuming, A.C., Hasebe, M., Lucas, S., Mishler, B.D., Reski, R., Grigoriev, I. V., Quatrano, R.S., Boore, J.L., 2008. The *Physcomitrella* Genome Reveals Evolutionary Insights into the Conquest of Land by Plants. *Science* (80-.). 319, 64–69. <https://doi.org/10.1126/science.1150646>

Resemann, H.C., 2018. Sphingolipids in *Physcomitrella patens*.

Resemann, H.C., Herrfurth, C., Feussner, K., Hornung, E., Ostendorf, A.K., Gömann, J., Mittag, J., van Gessel, N., Vries, J. de, Ludwig-Müller, J., Markham, J., Reski, R., Feussner, I., 2021. Convergence of sphingolipid desaturation across over 500 million years of plant evolution. *Nat. Plants* 7, 219–232. <https://doi.org/10.1038/s41477-020-00844-3>

Reski, R., Abel, W.O., 1985. Induction of budding on chloronemata and caulonemata of the moss, *Physcomitrella patens*, using isopentenyladenine, *Planta*. Springer-Verlag.

Roughan, P.G., Slack, C.R., Holland, R., 1978. Generation of phospholipid artefacts during extraction of developing soybean seeds with methanolic solvents. *Lipids* 13, 497–503. <https://doi.org/10.1007/BF02533620>

Sabovljević, M.S., Sabovljević, A.D., Ikram, N.K.K., Peramuna, A., Bae, H., Simonsen, H.T., 2016. Bryophytes – an emerging source for herbal remedies and chemical production. *Plant Genet. Resour.* 14, 314–327. <https://doi.org/10.1017/S1479262116000320>

Shanab, S.M.M., Hafez, R.M., Fouad, A.S., 2018. A review on algae and plants as potential source of arachidonic acid. *J. Adv. Res.* 11, 3–13. <https://doi.org/10.1016/j.jare.2018.03.004>

Tarazona, P., Feussner, K., Feussner, I., 2015. An enhanced plant lipidomics method based on multiplexed liquid chromatography-mass spectrometry reveals additional insights into cold- and drought-induced membrane remodeling. *Plant J.* 84, 621–633. <https://doi.org/10.1111/tpj.13013>

Tsugawa, H., Satoh, A., Uchino, H., Cajka, T., Arita, Makoto, Arita, Masanori, 2019. Mass Spectrometry Data Repository Enhances Novel Metabolite Discoveries with Advances in Computational Metabolomics. *Metabolites* 9, 119. <https://doi.org/10.3390/metabo9060119>

Valledor, L., Furuhashi, T., Hanak, A.-M., Weckwerth, W., 2013. Systemic Cold Stress Adaptation of *Chlamydomonas reinhardtii*. *Mol. Cell. Proteomics* 12, 2032–2047. <https://doi.org/10.1074/mcp.M112.026765>

Vu, H.S., Shiva, S., Roth, M.R., Tamura, P., Zheng, L., Li, M., Sarowar, S., Honey, S., McEllhiney, D., Hinkes, P., Seib, L., Williams, T.D., Gadbury, G., Wang, X., Shah, J., Welti, R., 2014. Lipid changes after leaf wounding in *Arabidopsis thaliana* : expanded lipidomic data form the basis for lipid co-occurrence analysis. *Plant J.* 80, 728–743. <https://doi.org/10.1111/tpj.12659>

Walker, A., Pfitzner, B., Harir, M., Schaubeck, M., Calasan, J., Heinzmann, S.S., Turaev, D., Rattei, T., Endesfelder, D., Castell, W. zu, Haller, D., Schmid, M., Hartmann, A., Schmitt-Kopplin, P., 2017. Sulfonolipids as novel metabolite markers of *Alistipes* and *Odoribacter* affected by high-fat diets. *Sci. Rep.* 7, 11047. <https://doi.org/10.1038/s41598-017-10369-z>

Wang, X., Li, W., Li, M., Welti, R., 2006. Profiling lipid changes in plant response to low temperatures. *Physiol. Plant.* 126, 90–96. <https://doi.org/10.1111/j.1399-3054.2006.00622.x>

Welti, R., Li, W., Li, M., Sang, Y., Biesiada, H., Zhou, H.-E., Rajashekar, C.B., Williams, T.D., Wang, X., 2002. Profiling Membrane Lipids in Plant Stress Responses. *J. Biol. Chem.* 277, 31994–32002. <https://doi.org/10.1074/jbc.M205375200>

Welti, R., Wang, X., Williams, T.D., 2003. Electrospray ionization tandem mass spectrometry scan modes for plant chloroplast lipids. *Anal. Biochem.* 314, 149–152. [https://doi.org/10.1016/S0003-2697\(02\)00623-1](https://doi.org/10.1016/S0003-2697(02)00623-1)

Zhang, X.D., Wang, R.P., Zhang, F.J., Tao, F.Q., Li, W.Q., 2013. Lipid profiling and tolerance to low-temperature stress in *Thellungiella salsuginea* in comparison with *Arabidopsis thaliana*. *Biol. Plant.* 57, 149–153. <https://doi.org/10.1007/s10535-012-0137-8>

Tables and figures

Table 1. Internal standard used for calculation of lipid relative concentration. PC, phosphatidylcholine; LPC, lysophosphatidylcholine; CE, cholesterol ester; MG, monodiacylglyceride; DG, diglyceride; TG, triglyceride; SM, sphingomyelin; Cer, ceramides; DGTS, diacylglycerol-N,N,N-trimethylhomoserine; PE, phosphatidylethanolamine; PS, phosphatidylserine; PG, phosphatidylglycerol; PI, phosphatidylinositol; LPE, lysophosphatidylethanolamine.

Compound	m/z	Adduct	Linear range (ug/mL)	Equation	R ²
PC 15:0 ₋ 18:1(d7)	753.6134	[M+H] ⁺	0.125-20	y = 278979x - 27702	0.9966
LPC 18:1(d7)	529.3993	[M+H] ⁺	0.125-20	y = 324275x - 26672	0.9947
CE 18:1(d7)	675.6779	[M+NH ₄] ⁺	5-40	y = 2465.4x - 7519.7	0.9943
MG 18:1(d7)	381.3704	[M+NH ₄] ⁺	1-40	y = 1582.3x + 240.42	0.9994
DG 15:0 ₋ 18:1(d7)	605.5845	[M+NH ₄] ⁺	0.125-40	y = 71212x + 3263.7	0.9925
TG 15:0 ₋ 18:1(d7) ₋ 15:0	829.7985	[M+NH ₄] ⁺	0.125-40	y = 281188x + 77072	0.9914

Compound	m/z	Adduct	Linear range (ug/mL)	Equation	R ²
SM 18:1;2O/18:1(d9)	738.6470	[M+H] ⁺	0.125-40	y = 159238x + 9945.7	0.9997
Cer 18:1;2O/15:0(d7)	531.5477	[M+H] ⁺	0.125-20	y = 278554x - 11784	0.9968
DGTS (d9)	721.6658	[M+H] ⁺	0.125-2.5	y = 2E+06x + 182473	0.995
PE 15:0_- 18:1(d7)	709.5519	[M-H] ⁻	0.125-20	y = 126515x + 800.14	0.9985
PS 15:0_- 18:1(d7)	753.5418	[M-H] ⁻	0.125-20	y = 57483x + 12403	0.9971
PG 15:0_- 18:1(d7)	740.5466	[M-H] ⁻	0.125-20	y = 213728x + 44408	0.9969
PI 15:0_- 18:1(d7)	828.5626	[M-H] ⁻	0.125-20	y = 162279x + 45604	0.9917
LPE 18:1(d7)	485.3378	[M-H] ⁻	0.125-20	y = 194625x + 5032.5	0.9961

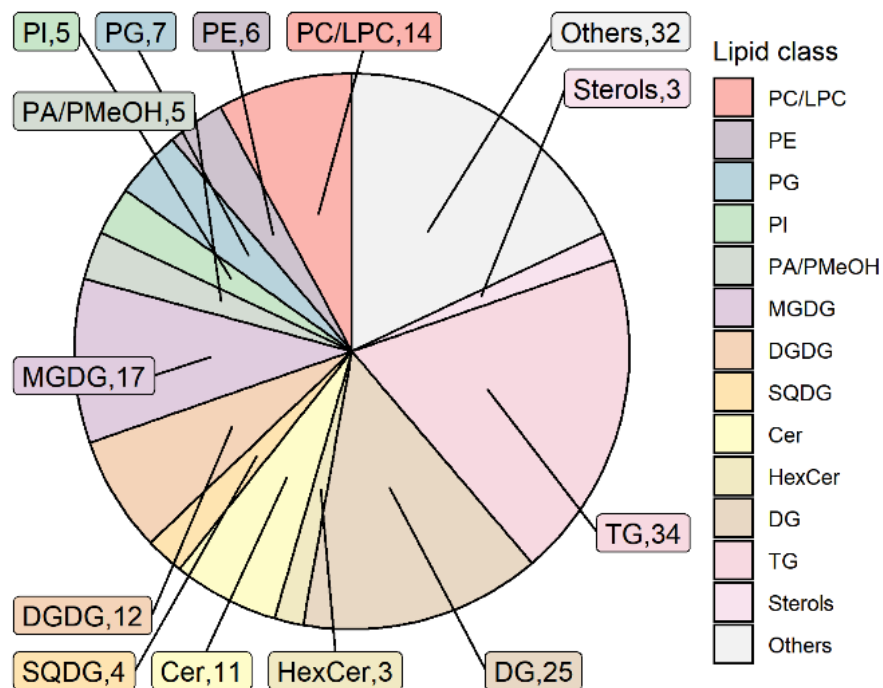


Figure 1. Detected lipid classes and the numbers of lipid molecular species in (A). *B. pseudotriquetrum* in ESI+, (B). *P. patens* in ESI+, (C). *B. pseudotriquetrum* in ESI-, and (D) *P. patens* in ESI-. PC, phosphatidylcholine; LPC, lysophosphatidylcholine; PE, phosphatidylethanolamine; PG, phosphatidylglycerol; PI, phosphatidylinositol; PA, phosphatidic acid; PMeOH, phosphatidylmethanol; MGDG, monogalactosyldiacylglycerol; DGDG, digalactosyldiacylglycerol; SQDG, sulfoquinovosyldiacylglycerol; Cer, ceramides; HexCer, hexosylceramide; DG, diglyceride; TG, triglyceride; SL, sulfonolipid; FA, fatty acids

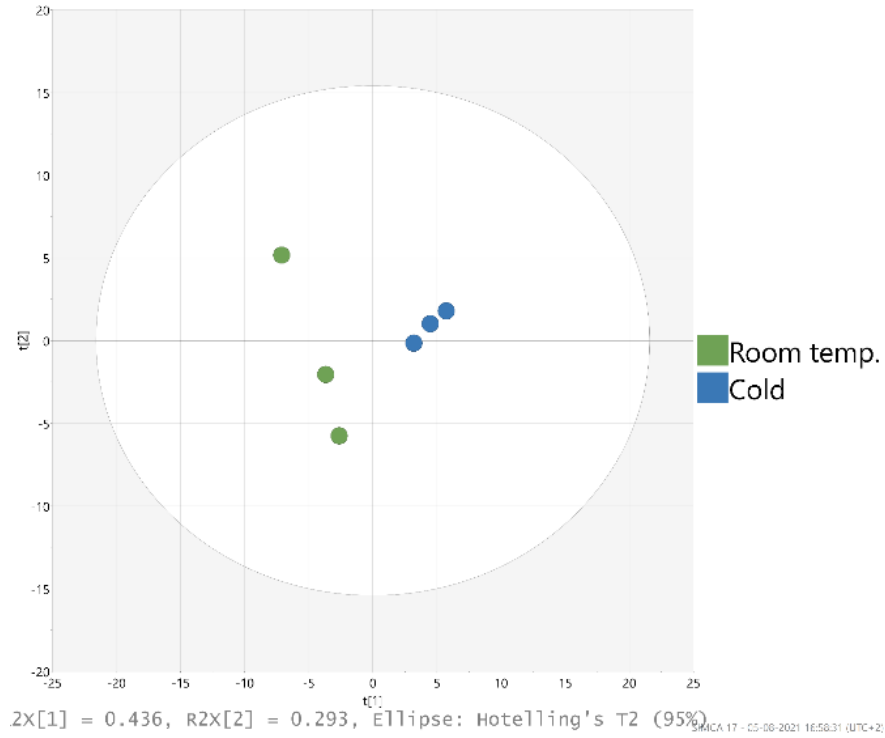


Figure 2. PLS-DA score plot of *B. pseudotriquetrum* at room temperature and under cold stress in ESI+ mode (A) ($R^2X = 0.449$, $R^2Y = 0.997$, $Q^2Y = 0.676$) and in ESI- mode (B) ($R^2X = 0.728$, $Q^2Y=0.961$, $Q^2=0.804$), *P. patens* at room temperature and under cold stress in ESI+ mode (C) ($R^2X = 0.768$, $R^2Y = 0.986$, $Q^2 = 0.693$) and in ESI- mode (D) ($R^2X = 0.893$, $R^2Y = 0.969$, $Q^2 = 0.740$).

10 (dark green). T-test was performed to calculate the significant differences (-: $p > 0.05$, *: $p \leq 0.05$, **: $p \leq 0.01$, ***: $p \leq 0.001$) and error bars indicate the standard deviation of three replicates. PC, phosphatidylcholine; PE, phosphatidylethanolamine; PG, phosphatidylglycerol; PI, phosphatidylinositol; PA, phosphatidic acid; MGDG, monogalactosyldiacylglycerol; DGDG, digalactosyldiacylglycerol; SQDG, sulfoquinovosyldiacylglycerol. DG, diglyceride; TG, triglyceride; Cer, ceramides; PMeOH, phosphatidylmethanol; LPC, lysophosphatidylcholine; SL, sulfonolipid. The quantification of lipids were calculated by using internal standards representing each lipid classes with a few exceptions, PA, was normalized by Cer 18:1;2O/16:0(d7), and MGDG, DGDG, and SQDG were normalized by DGTS d9.